Macromolecules
ARTICLE

Macromolecules **2009**, *42*, 7563–7570 **7563**
DOI: 10.1021/ma901111w

Interactions between Surfaces in Polydisperse Semiflexible Polymer Solutions

Clifford E. Woodward*,† and Jan Forsman*,‡

†*School of Physical, Environmental and Mathematical Sciences University College, University of New South Wales, ADFA Canberra ACT 2600, Australia, and* ‡*Theoretical Chemistry, Chemical Centre P.O.Box 124, S-221 00 Lund, Sweden*

Received May 21, 2009; Revised Manuscript Received August 19, 2009

ABSTRACT: We generalize a recently developed polymer density functional theory (PDFT) for polydisperse polymer fluids to the case of semiflexible (stiff) polymers. As with our earlier work on flexible polymers, we show here that the generalization of the PDFT to polydisperse mixtures of semiflexible chains allows us to obtain a remarkable simplification of the solution algorithm, compared to the monodispersed case. The number of required equations for complete solution of the (polydisperse) PDFT scales inversely with the *width* of the polydispersity profile. This reflects the fact that more information is required, the narrower is the polydispersity. We apply the theory to a number of model scenarios, including repulsive and adsorbing surfaces. We find that polydispersity effects on the depletion interaction are larger for dilute solutions and when the surfaces are adsorbing. We also investigate short, stiff chains and find rather dramatic effects in the presence of adsorbing surfaces.

Introduction

Polymers have a profound effect on interactions between surfaces. This property finds application in many industrial and biological phenomena, such as colloidal stability and protein crystallization.[1,2] Polymer density functional theory, PDFT, has proven to be a powerful theoretical tool for the treatment of these kinds of systems.[3−7]

Density functional calculations to date have almost exclusively focused on monodispersed chains. This is despite the fact that laboratory samples of polymers rarely possess chains of a single molecular weight. In recent years, polydispersity has come to be viewed as a potentially useful experimental variable, that can be used to alter the effect that polymers have on surface interactions. This has made it desirable to find theoretical treatments for polydisperse systems. Recently, Yu et al.[8] have used density functional theory to study polydisperse hard sphere fluids. This model finds limited applicability for polymers in good solvents. More relevant are other treatments for polymer fluids. For example, Tuinier and Pethukhov used a product function approximation to study polydispersity effects on depletion by ideal chains.[9] The special case of equilibrium polymers has been rather thoroughly analyzed by van der Gucht and co-workers.[10−13] Additionally, Scheutjens-Fleer theory[14] has been applied to polydisperse polymers at surfaces.[15] There have also been recent attempts to treat more general molecular weight distributions with Edwards−de Gennes self-consistent-field theory, SCF,[16−18] wherein the effect of polydispersity has been numerically integrated within the solution algorithm using adapted quadrature methods.[19−21] These methods were originally devised to consider effects of polydispersity on bulk phase diagrams. However, recent work by Yang et al.[22] studied the effect of polydispersity on the depletion interaction between nonadsorbing surfaces. They found that the effects of polydispersity on surface interactions were relatively modest. This may be, primarily, a consequence of the flexible chain models used in those studies and/or the concentrated solution regime in which the calculations were performed. The mean-field nature of PDFT makes the concentrated regime preferable. This notwithstanding, in this work, we will perform some speculative calculations in more dilute solutions, that suggest polydispersity effects can become more significant when the concentration is reduced. In general, much larger effects on surface forces are found in solutions of semiflexible chains, especially as the degree of stiffness is increased. For example, chain stiffness will cause both the range and strength of attractive depletion forces, between nonadsorbing surfaces, to increase significantly. On the other hand, if surfaces are made attractive to polymers, a significant repulsive barrier appears in the surface interaction, due to the steric interactions between chains adsorbed on the opposing surfaces. This barrier becomes larger and occurs at greater surface separation, the more stiff the chains are. Thus, introducing polydispersity into a solution of semiflexible polymers may have a more significant effect on the resulting surface forces. For example, polydispersity might be expected to attenuate repulsive surface interactions and enhance attractive ones, as the system now has an extra degree of freedom with which it can minimize the free energy.

The solution of PDFT for semiflexible polymer models has greater computational requirements than comparable calculations for flexible chains. These requirements still scale linearly with the length of the polymer, but the number of numerical operations required increases significantly per additional monomer, as compared with the flexible model. This is because next-nearest neighbor interactions come into play, requiring storage of higher dimensional (albeit sparse) matrices. Established theoretical methods for treating polydispersity, as described above, would usually increase the computational demands, dramatically for wide distributions. Recently, however, we showed how the PDFT could be easily generalized to include polydispersity, in the case where the molecular weight distribution is of the Schulz−Flory (Zimm) form.[23] Quite surprisingly, we found that

*Corresponding authors. E-mail: (C.E.W.) c.woodward@adfa.edu.au; (J.F.) jan.forsman@teokem.lu.se.

Published on Web 09/18/2009

the algebraic structure of the PDFT was simpler than that for the monodispersed fluid. Furthermore, this manifested itself in a numerically more efficient solution algorithm. The formalism we derived was for flexible polymers. The aims of this article are 2-fold. First, we generalize of the polydisperse density functional theory to semiflexible polymer models. Second, we apply that theory to study polydispersity effects on surface forces.

Theory

Density Functional Theory for Polydisperse Semi-Flexible Polymers. In our derivation, we shall use the general formulation due to Woodward.[3] Most versions of the PDFT either use a similar approach, or can be recast as such. The derivation of a PDFT for semiflexible polymers can be found in reference.[24] We briefly outline aspects of that derivation which are of relevance for the application to *polydisperse* semiflexible polymers.

The exact canonical free energy density functional, F_r^{id}, for an ideal, semiflexible r-mer polymer fluid is given by

$$\beta F_r^{id} = \int d\mathbf{R}\, N_r(\mathbf{R})(\ln[N_r(\mathbf{R})]-1)+\int d\mathbf{R}\, N_r(\mathbf{R})\Phi^{(b)}(\mathbf{R}) + \int d\mathbf{r}\, n_r(\mathbf{r})\psi^0(\mathbf{r})+\int d\mathbf{R}\, N_r(\mathbf{R})\sum_{i=1}^{r-2} E_B(\mathbf{s}_i,\mathbf{s}_{i+1}) \quad (1)$$

where β is the inverse thermal energy. The r-point density, $N_r(\mathbf{R})$, is a function of the monomer configuration $\mathbf{R} = (\mathbf{r}_1, ..., \mathbf{r}_r)$, where $\mathbf{r}_i$ is the coordinate of monomer i. The potential $\Phi^{(b)}(\mathbf{R})$ describes the intramolecular connectivity constraints, manifested by a nearest-neighbor, nondirectional bonding, i.e.,

$$\Phi^{(b)}(\mathbf{R}) = \sum_{i=1}^{r-1}\phi^{(b)}(|\mathbf{r}_i-\mathbf{r}_{i+1}|) \quad (2)$$

The bending potential, E_B, introduces a degree of stiffness into the polymer molecules. We assume the following form for this potential,

$$\beta E_B(\mathbf{s}_i,\mathbf{s}_{i+1}) = \varepsilon\left(1-\frac{\mathbf{s}_i\cdot\mathbf{s}_{i+1}}{\sigma^2}\right) \quad (3)$$

where, $\mathbf{s}_i$, denotes the bond vector between monomers i and $i+1$, i.e., $\mathbf{s}_i = \mathbf{r}_{i+1} - \mathbf{r}_i$, and ε is the strength of the bending potential. All monomers in the chain are assumed to interact indentically with the external potential, $\psi^0(\mathbf{r})$. For fluids with additional nonbonding interactions, the ideal functional, eq 2, must be supplemented with a suitable excess term, F^{ex}. A common assumption for most versions of PDFT, and that which will be adopted here, is that F^{ex} is a functional only of the total monomer density, $n_m(\mathbf{r})$.

We consider now a grand canonical ensemble system, whereby a bulk fluid, which determines the chemical potential, consists of a polydisperse sample of polymer. The chemical potential of the r-mer in the bulk is denoted as, μ_r. It is given by the expression,

$$\beta\mu_r = \ln[\phi_p F(r)]+\beta\mu^{ex} \quad (4)$$

Here ϕ_p is the total bulk density of polymer molecules and μ^{ex} is the excess chemical potential of the r-mer. The latter is ultimately determined by the equation of state used in the model whereby it is usually approximated as being linearly dependent on r. $F(r)$, is the normalized, molecular weight distribution of the bulk fluid. In this work, $F(r)$, will be described using the well-known Schultz−Flory (S−F) distribution,

$$F(r) = Kr^n e^{-\kappa r} \quad (5)$$

where

$$K = \left(\frac{n+1}{\langle r\rangle_b}\right)^{n+1}\frac{1}{\Gamma(n+1)} \quad (6)$$

$$\kappa = \frac{n+1}{\langle r\rangle_b} \quad (7)$$

$\Gamma(x)$ is a gamma function and $\langle r\rangle_b$ is the average degree of polymerization of the bulk solution. The quantity, $\lambda = n+1$, determines the width of the distribution. The case $\lambda = 1$ corresponds to equilibrium (living) polymers, and as λ increases the polydispersity distribution becomes narrower. As in our earlier work, we shall assume that λ is an integer.

The total grand potential functional, Ω, for the *polydisperse* polymer fluid is given by

$$\Omega = \sum_r F_r^{id}[N_r(\mathbf{R})]+F^{ex}[n_m(\mathbf{r})]-\sum_r \mu_r\int d\mathbf{R}\, N_r(\mathbf{R}) \quad (8)$$

Minimizing the grand free energy with respect to $N_r(\mathbf{R})$ gives the following integral equation,

$$N_r(\mathbf{R}) = \phi_p F(r)\prod_{i=1}^{r-1} T(|\mathbf{r}_i-\mathbf{r}_{i+1}|)\prod_{i=1}^{r-2}\Psi(\mathbf{r}_i,\mathbf{r}_{i+1},\mathbf{r}_{i+2})\prod_{i=1}^{r} e^{-\psi(\mathbf{r}_i)} \quad (9)$$

The presence of the stiffness correlation term, $\Psi(\mathbf{r}_i,\mathbf{r}_{i+1},\mathbf{r}_{i+2})$, introduces a next nearest neighbor interaction. It is given by,

$$\Psi(\mathbf{r}_i,\mathbf{r}_{i+1},\mathbf{r}_{i+2}) = e^{-\beta E_B(\mathbf{s}_i,\mathbf{s}_{i+1})} \quad (10)$$

The mean-field also includes a contribution from the monomer excess chemical potential, μ_{mon}^{ex}, which implies that the mean-field is zero in the bulk fluid.

$$\psi(\mathbf{r}) \equiv \frac{\delta\beta F^{ex}}{\delta n(\mathbf{r})}+\psi^0(\mathbf{r})-\beta\mu_{mon}^{ex} \quad (11)$$

The bonding kernel, $T(|\mathbf{r}_i\text{-}\mathbf{r}_{i+1}|)$, is given by,

$$T(|\mathbf{r}_i-\mathbf{r}_{i+1}|) = e^{-\phi^{(b)}(|\mathbf{r}_i-\mathbf{r}_{i+1}|)} \quad (12)$$

The explicit form for this bonding potential does not affect the general derivation below. In our calculations, however, we will use a simple form, wherein monomers are bound at a fixed distance equal to their diameter σ. Thus,

$$T(|\mathbf{r}-\mathbf{r}'|) = \delta(|\mathbf{r}-\mathbf{r}'|-\sigma) \quad (13)$$

where a normalization factor is appropriately incorporated into the bulk chemical potential. From eq 9, one can obtain the total average monomer density,

$$n_m(\mathbf{r}) = \sum_{r=1}^{\infty}\int d\mathbf{R}\,\sum_{i=1}^{r}\delta(|\mathbf{r}-\mathbf{r}_i|)N_r(\mathbf{R}) \quad (14)$$

It is convenient to introduce chain propagator functions, which satisfy the following recursion formula,

$$c(i;\mathbf{r}',\mathbf{r}) = \mathrm{e}^{-\psi(\mathbf{r}')}\int c(i-1,\mathbf{r}'',\mathbf{r}')T(|\mathbf{r}'-\mathbf{r}|)\Psi(\mathbf{r}'',\mathbf{r}',\mathbf{r})\,\mathrm{d}\mathbf{r}'' \tag{15}$$

with boundary condition $c(0;\mathbf{r}',\mathbf{r}) = 1$. We note that the arguments $\mathbf{r}'$ and $\mathbf{r}$ in the $c(i;\mathbf{r}',\mathbf{r})$, are ordered. In terms of these functions, the monomer density can be recast into the following useful form,

$$n_m(\mathbf{r}) = \phi_p\sum_{r=1}^{\infty}F(r)\sum_{i=1}^{r}\int \mathrm{d}\mathbf{r}'\,c(r-i;\mathbf{r}',\mathbf{r})T(|\mathbf{r}-\mathbf{r}'|)c(i;\mathbf{r},\mathbf{r}')\,\mathrm{d}\mathbf{r}' \tag{16}$$

Equations 11−16 form a closed set of equations to be solved self-consistently. In its current form, the solution to the polydispersity problem requires the self-consistent determination of r propagator functions for each r-mer in the distribution. As the distribution is continuous, it would appear that one would need to discretize it, providing a finite quadrature approximation to integration over the distribution. This approach has been used in several self-consistent field (SCF) applications,[19,20] where it has been shown that adaptive quadrature methods can lead to efficiently evaluated approximations. However, this approach generally leads to more expensive and complex solution algorithms, when compared with a typical calculations for a monodispersed polymer fluid. In previous work, we have already shown (for flexible polymers), that the form of the S−F distribution affords a more straightforward (and elegant) solution to the problem.[23] Below we shall demonstrate how a similar approach can be applied to semiflexible polymers. We also note that, due a simple reformulation of terms, the relations derived below are even simpler than those which appeared in our earlier work.

We begin by substituting the explicit form of the S−F distribution into eq 16, which gives

$$\begin{aligned} n_m(\mathbf{r}) &= \phi_p K\sum_{r=1}^{\infty}\sum_{i=1}^{r}r^n\mathrm{e}^{-\kappa r}\int \mathrm{d}\mathbf{r}'\,c(r-i;\mathbf{r}',\mathbf{r})T(|\mathbf{r}-\mathbf{r}'|)c(i;\mathbf{r},\mathbf{r}') \\ &= \phi_p K\sum_{r=1}^{\infty}\sum_{i=1}^{r}(r-i+i)^n\mathrm{e}^{-\kappa(r-i)}\int \mathrm{d}\mathbf{r}'\,c(r-i;\mathbf{r}',\mathbf{r}) \\ &\quad\times T(|\mathbf{r}-\mathbf{r}'|)\mathrm{e}^{-\kappa i}c(i;\mathbf{r},\mathbf{r}') \\ &= n!\phi_p K\sum_{l=0}^{n}\sum_{r=1}^{\infty}\sum_{i=1}^{r}\int \mathrm{d}\mathbf{r}'\,\frac{(r-i)^l}{l!}\mathrm{e}^{-\kappa(r-i)}c(r-i;\mathbf{r}',\mathbf{r}) \\ &\quad\times T(|\mathbf{r}-\mathbf{r}'|)\frac{i^{n-l}}{(n-l)!}\mathrm{e}^{-\kappa i}c(i;\mathbf{r},\mathbf{r}') \end{aligned} \tag{17}$$

The double sum over r and i can be carried out, being careful to treat the term $i = r$ as a special case (which includes the $r = 1$ term). We are led to the very simple equation,

$$\begin{aligned} n_m(\mathbf{r})/\phi_p K n! &= \sum_{l=0}^{n}\int \mathrm{d}\mathbf{r}'\,\hat{c}(l;\mathbf{r}',\mathbf{r})T(|\mathbf{r}-\mathbf{r}'|)\hat{c}(n-l;\mathbf{r},\mathbf{r}') \\ &\quad+\int \mathrm{d}\mathbf{r}'T(|\mathbf{r}-\mathbf{r}'|)\hat{c}(n;\mathbf{r},\mathbf{r}') \end{aligned} \tag{18}$$

where the transformed propagators are defined by,

$$\hat{c}(k;\mathbf{r},\mathbf{r}') = \sum_{i=1}^{\infty}\mathrm{e}^{-\kappa i}i^k c(i;\mathbf{r},\mathbf{r}')/k! \tag{19}$$

Thus, the multiple sum in eq 16 is replaced by a much smaller sum of terms in eq 18 involving only $n + 1$ transformed propagators. However, we still require a closed expression for the transformed propagators. This can be obtained by multiplying both sides of eq 15 by $(i+1)^l e^{-\kappa(i+1)}/l!$ and summing over i. The following recursion formula results,

$$\begin{aligned} \hat{c}(l;\mathbf{r}',\mathbf{r}) &= \mathrm{e}^{-\psi(\mathbf{r}')}\mathrm{e}^{-\kappa}\left\{\sum_{m=0}^{l}\frac{1}{(l-m)!}\right. \\ &\quad\left.\times\int \mathrm{d}\mathbf{r}''\,\hat{c}(m;\mathbf{r}'',\mathbf{r}')T(|\mathbf{r}''-\mathbf{r}'|)\Psi(\mathbf{r}'',\mathbf{r}',\mathbf{r})+1\right\} \end{aligned} \tag{20}$$

which is closed by the initial condition,

$$\hat{c}(0;\mathbf{r}',\mathbf{r}) = \mathrm{e}^{-\psi(\mathbf{r}')}\mathrm{e}^{-\kappa}\left\{\int \mathrm{d}\mathbf{r}''\,\hat{c}(0;\mathbf{r}'',\mathbf{r}')T(|\mathbf{r}''-\mathbf{r}'|)\Psi(\mathbf{r}'',\mathbf{r}',\mathbf{r})+1\right\} \tag{21}$$

Model and Adsorption Potentials. As noted earlier, different versions of PDFT arise from the choice of the excess functional, F^{ex}.[3−7,25−31] Thus, far we have developed the theory assuming that the solvent molecules only enters implicitly, via the monomer−monomer potential of mean force. It is straightforward to generalize the approach to polymer *solutions* with an explicit solvent, however, we shall remain with an implicit solvent model in this study. Here, we employ the generalized Flory dimer expression for monomer−monomer hard core interactions,[4,27] which means that we are assuming good solvent conditions.

In order to illustrate typical effects due to the combination of polydispersity and stiffness, we investigate the interaction between two flat and infinite surfaces, immersed in a polymer solution. The interaction between the surfaces and monomers is given by $V_0(z,h) = w(z) + w(h - z)$. where $w(z)$ is a truncated and shifted Lennard-Jones potential, i.e., $w(z) = w_{LJ}(z) - w_{LJ}(z_c)$, for $z < z_c$, and zero otherwise. Here,

$$\beta w_{L\text{-}J}(z) = 2\pi\left[\frac{2}{45}\left(\frac{\sigma}{z}\right)^9 - \frac{a_w}{3}\left(\frac{\sigma}{z}\right)^3\right]$$

and we have set $z_c = 4\sigma$. An *adsorbing* surface is characterized by $a_w = 1$, while $a_w = 0$ creates a *nonadsorbing* surface. In order to avoid trivial effects due to the surface−surface interaction, we have only investigated separations at which there is no overlap between the potentials from either surface, i.e., $h > 8\sigma$.

The planar symmetry of the system allows a simplification of the bending contribution to the polymer distribution. With $\Delta z_i \equiv z_{i+1} - z_i$, we can write the vector product between adjacent bond vectors as

$$\mathbf{s}_i\cdot\mathbf{s}_{i+1} = \Delta z_i\Delta z_{i+1} + (\sigma^2 - \Delta z_i^2)^{1/2}(\sigma^2 - \Delta z_{i+1}^2)^{1/2}\cos\phi_{i,i+1} \tag{22}$$

where $\phi_{i,i+1}$ is the angle between $\mathbf{s}_i$ and $\mathbf{s}_{i+1}$, as projected onto the plane of the surfaces. If we average the corresponding Boltzmann factor over the surface plane, we get,

$$\begin{aligned} &\Psi(\Delta z_i, \Delta z_{i+1}) \\ &= \mathrm{e}^{-\varepsilon(1-\Delta z_i\Delta z_{i+1}/\sigma^2)}I_0\left[\varepsilon\left(1-\left(\frac{\Delta z_i}{\sigma}\right)^2\right)^{1/2}\left(1-\left(\frac{\Delta z_{i+1}}{\sigma}\right)^2\right)^{1/2}\right] \end{aligned} \tag{23}$$

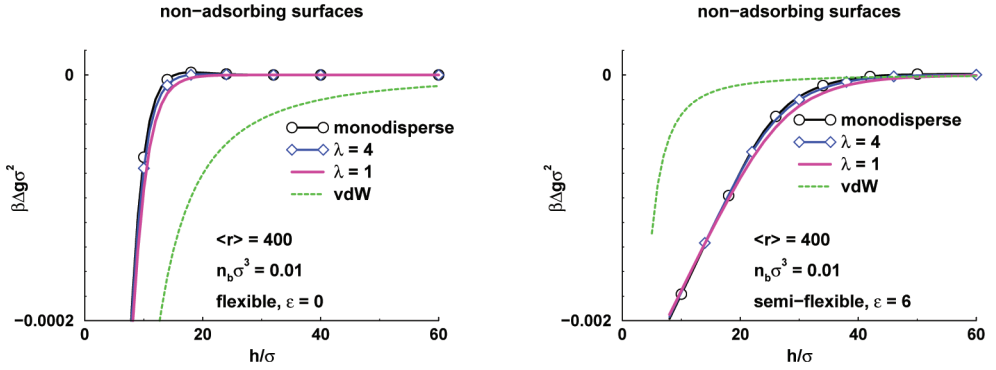

Figure 1. Interaction free energies per unit area (Δg), between nonadsorbing surfaces, immersed in polymer solutions containing chains with an average length, $\langle r \rangle_b = 400$. The bulk monomer concentration is $n_b\sigma^3 = 0.01$. (a) Flexible polymers, with varying degrees of polydispersity. (b) Semiflexible polymers, $\varepsilon = 6$, with varying degrees of polydispersity.

where

$$I_0(x) = \frac{1}{2\pi}\int_0^{2\pi} \exp[-x\cos\phi]\, d\phi$$

is a modified Bessel function, which can be evaluated from a polynomial expansion.

Unless otherwise stated, the total bulk monomer density, n_b, is set to $0.01/\sigma^3$. The net free energy per unit area, $g(h)$, is given by $g(h) = \Omega_{eq}/S + P_b h$ where Ω_{eq} is the equilibrium grand potential and P_b is the osmotic pressure in the bulk. The net interaction free energy, which is plotted in the figures below, is obtained by removing the bulk surface terms at inifinte separation of the surfaces, i.e., $\Delta g(h) = g(h) - g(\infty)$.

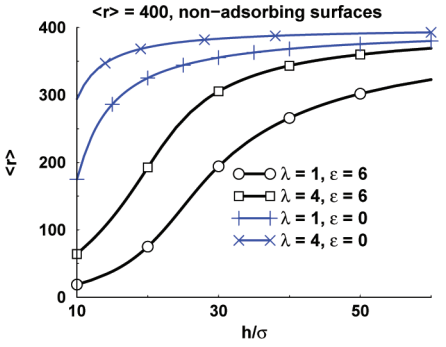

Figure 2. The average polymer length, $\langle r \rangle$, of chains in the intersurface (slit) region. Polymer solutions were as defined in Figure 1.

Results

Semiflexible Polymers, Nonadsorbing Surfaces. Here we consider polymer solutions in contact with nonadsorbing surfaces. This system is similar to results reported by Yang et al.[22] However, in their case, theta conditions were assumed. Parts a and b of Figure 1 show the interaction between surfaces for a fully flexible polymer ($\varepsilon = 0$) and a stiffer polymer model ($\varepsilon = 6$), as a function of the degree of polydispersity. A typical hydrocarbon−water-hyrocarbon dispersion interaction (Hamaker constant: 5×10^{-21} J) is also shown for comparison. These interaction curves display typical depletion attraction. Reduction of the configurational entropy of the polymers due to the surfaces cause a diminished average density between the surfaces, leading to a greater osmotic attraction between the surfaces as they approach. For the stiffer polymers, this mechanism leads to surface interactions which are much larger, both in range and magnitude. However, for both stiff and flexible models the qualitative effect of introducing polydispersity is rather small. This notwithstanding, it is still worthwhile exploring the changes that occur upon going to a polydisperse sample. For example, there is a discernible increase in the range of the attraction between the surfaces as the polydispersity index increases (λ decreases). This is due to a decrease in the relative number of longer polymers between the surfaces, as h decreases. The system obviously minimizes the free energy by increasing the proportion of shorter polymers between the surfaces, as their configurational entropy is less affected by the walls. The depletion of polymers longer than the average molecular weight(present in polydisperse samples) leads to an osmotic attraction at quite larger separations, compared with the monodispersed case. Figure 2 shows that the average polymer length in the slit, $\langle r \rangle$, is smaller than its bulk value, even at rather large separations. Not surprisingly, this effect is greater for the stiffer polymers at larger separation, as they have a larger radius of gyration. However, at shorter separations, the rate of decrease in $\langle r \rangle$ with separation is smaller for semiflexible polymers. This is because stiffer chains lose less configurational entropy than their flexible counterparts, once the surface separation is much shorter than their respective radii of gyration. The relative increase in the number of short polymers between the surfaces, as the separation decreases, is greater for samples with higher polydispersity. For example, the average polymer length has diminished to approximately 15 for stiff polymers with $\lambda = 1$ at a separation of $h = 10\sigma$. It is four times larger for $\lambda = 4$, at the same separation. Nevertheless, as noted above, the consequent changes to the interaction free energies are small. That is, at large separations, the osmotic pressure for polydisperse systems is only slightly more attractive than for the monodispersed case, with a discernible crossover occurring at smaller separations. The crossover occurs because monodispersed polymers are now significantly depleted from between the surfaces, while in the polydisperse case the number of shorter polymers between the surfaces creates a relatively more repulsive osmotic pressure. This leads to a relatively larger free energy as the configurational entropy of these shorter polymers is reduced by the surfaces. Though polydispersity effects appears to be small under these conditions, it is well-known that if the monomer concentration is high enough, excluded volume effects on the correlation length can be significant. That is, monomer correlations become screened and the surface interaction can become relatively insensitive to chain length. At considerably lower concentrations, the range of the depletion attraction is essentially governed by the radius of gyration. Hence, effects from polydispersity are expected to be more pronounced.

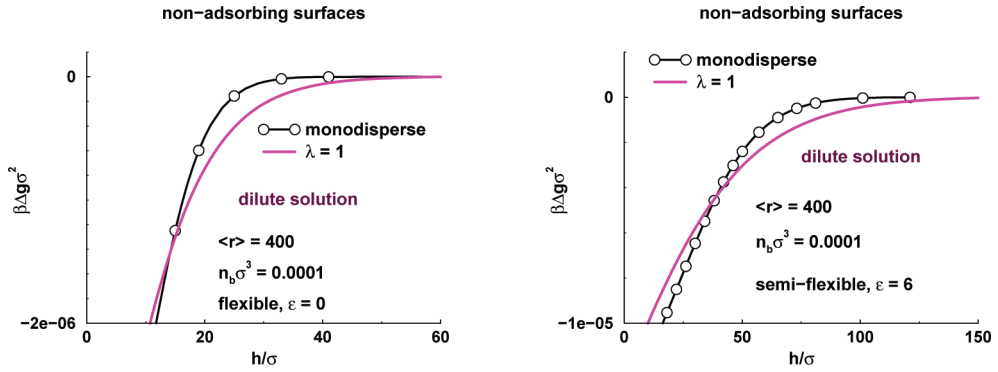

Figure 3. Interaction free energies per unit area, between nonadsorbing surfaces, immersed in polymer solutions containing chains with an average length in the bulk, $\langle r \rangle_b = 400$. The bulk monomer concentration is $n_b\sigma^3 = 0.0001$, i.e. considerably lower than in Figure 1. (a) Flexible polymers, with varying degrees of polydispersity. (b) Semiflexible polymers, $\varepsilon = 6$, with varying degrees of polydispersity.

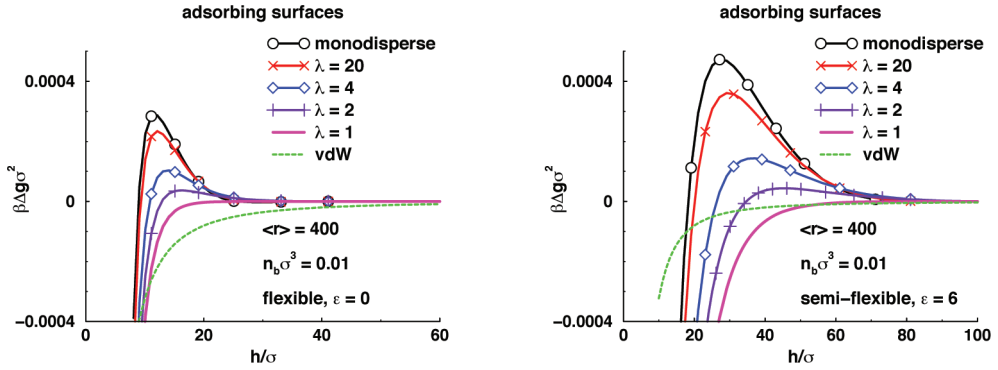

Figure 4. Interaction free energies per unit area, between adsorbing surfaces, immersed in polymer solutions containing chains with an average length in the bulk given by, $\langle r \rangle_b = 400$. The bulk monomer concentration is $n_b\sigma^3 = 0.01$. (a) Flexible polymers, with varying degree of polydispersity. (b) Semiflexible polymers, $\varepsilon = 6$, with varying degree of polydispersity.

This is verified by the results in Figure 3 wherein the polymer concentration is reduced 100-fold. In this case, the range of the depletion attraction increases considerably with the width of the molecular weight distribution.

Semiflexible Polymers, Adsorbing Surfaces. Parts a and b of Figure 4 show the interaction between two surfaces that adsorb monomers via a truncated L-J interaction, as described earlier. The general shape of the interaction free energy curves is qualitatively different to the depletion interaction between nonadsorbing walls. Also, we again see that the introduction of polymer stiffness into the model increases both the strength and the range of the interaction. Making the surfaces attractive to monomers has introduced a barrier into the free energy. The presence of this barrier has already been noted by us in previous work.[31−33,35,36] It is due to the steric interaction experienced between the tails of the adsorbed polymer layers on each surface. For the stiffer polymers investigated here ($\varepsilon = 6$), the tails of adsorbed polymers generally project further than for flexible polymers. Thus, the barrier occurs at larger separation for the stiffer polymers. On the other hand, as the surfaces approach one another, penetration of tails to the other surface occurs and attractive bridging interactions begin to dominate, leading to a strong attraction at shorter separation.

Surfaces which are attractive to monomers, provide a different mechanism by which polydisperse polymers can lower their free energy. Unlike the case of nonadsorbing walls, longer polymers will tend to adsorb more strongly between attractive surfaces in polydisperse samples due to cooperative adsorption between monomers. This cooperativity is greater for stiffer polymers, which lose less

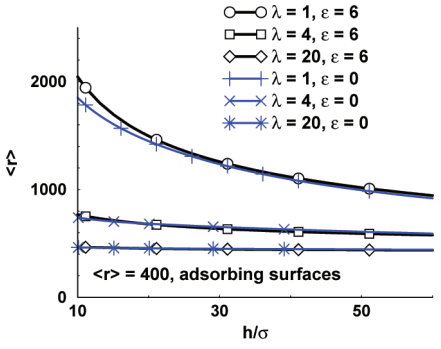

Figure 5. Average polymer length of chains in the intersurface (slit) region. Polymer solutions as defined in Figure 4.

configurational entropy when they adsorb onto surfaces, than their flexible counterparts. Thus, for polydisperse systems in general, the average molecular weight of polymers between the surfaces is larger than that of the bulk. This occurs at all separations, as shown in Figure 5. Not surprisingly, the more widely polydisperse samples allow adsorption of longer polymers. For example, equilibrium polymers ($\lambda = 1$) between the surfaces have an average length some five times higher (at separation $h = 10\sigma$) than in the bulk. Generally, the average polymer length between the surfaces increases as the surfaces approach. As the average length of the adsorbed chains becomes larger, the bridging attraction concomitantly increases. It is the ability of longer polymers to bridge between surfaces, at relatively small cost to their configurational entropy, which leads to their preferential

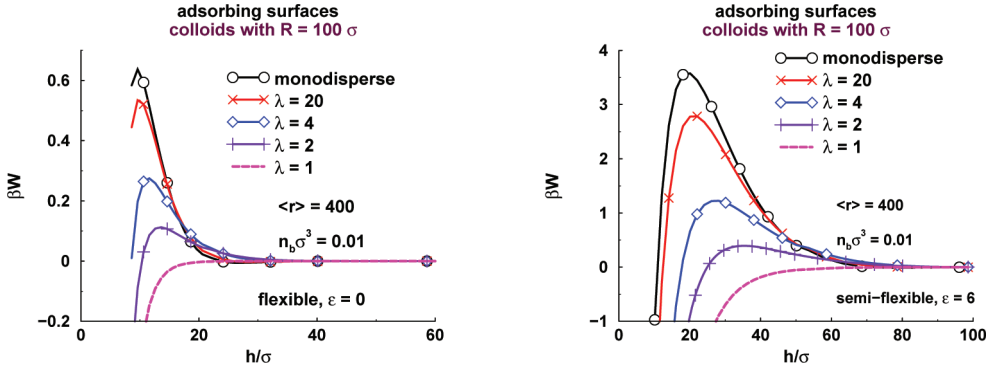

Figure 6. Interaction free energies (W), between adsorbing spherical colloids, as obtained via the Derjaguin approximation, eq 24, assuming a colloid radius of 100 σ. The bulk monomer density is $n_b\sigma^3 = 0.01$. (a) Flexible polymers, with varying degree of polydispersity. (b) Semiflexible polymers, $\varepsilon = 6$, with varying degree of polydispersity.

accumulation in the region at and between the surfaces. The increased bridging strength leads to a reduction of the free energy barrier, as clearly seen in Figure 4, parts a and b. Again, this effect is stronger for stiffer chains. One interesting result is that for equilibrium polymers, the free energy barrier appears to have disappeared completely. Compared with the case of depletion attraction between nonadsorbing surfaces, the effect of both stiffness *and polydispersity* on the interaction free energies are relatively much larger. It is interesting to conjecture upon the variation of the effects discussed above. In polydisperse systems, a purely repulsive surface enhances the adsorption of shorter chains. For attractive surfaces, longer chains are favored. Presumably there is a crossover behavior at an intermediate adsorption strength. At this point the adsorption strength is able to compensate for the loss in configurational entropy of chains to some extent.

In order to determine if the magnitude of the polymer mediated forces (shown in Figure 4, parts a and b) are relevant to phenomena such as colloidal stability, we have employed the Derjaguin approximation.[37] This allows us to estimate the interaction between large nanoparticles. Specifically, Derjaguin derived the following expression for the interaction between two spherical colloidal particles, with radius R

$$W(D) \approx -\pi R \int_D^\infty \mathrm{d}x\, g(x) \qquad (24)$$

where $g(x)$ is the free energy per unit area between the surfaces, and D is the surface to surface separation between the spheres. Recent work by us has shown that the Derjaguin approximation can be quite accurate, even for surprisingly small colloidal radii (relative to that of the polymer radius of gyration).[38] We chose a sphere radius of 100σ. The resulting interactions, under adsorbing conditions, are presented in Figure 6. The free energy barrier is about $0.6k_BT$ for monodispersed flexible polymers, and $3.5k_BT$ for monodispersed stiff polymers. Note also that the barrier occurs at larger separation in the latter case, which makes the barrier more relevant. This is because the van der Waals attraction rapidly becomes weak as the separation increases.

The most important effect of polydispersity is the progressive diminishing of this free energy barrier, as the samples are made more polydisperse, to the point of monotonic attraction, in the presence of equilibrium polymers. These barriers seem to contradict a well-known theorem by de Gennes, according to which surface interactions at full equilibrium, always are monotonically attractive.[18]

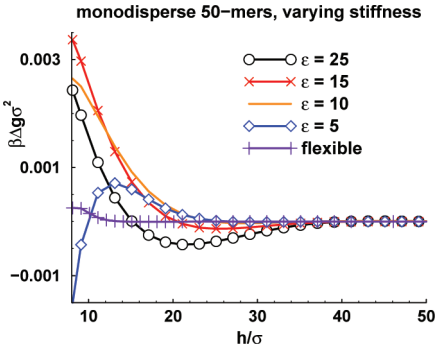

Figure 7. Interaction free energies per unit area, between adsorbing surfaces, immersed in monodisperse polymer solutions, where $r = 50$. The bulk monomer concentration is $n_b\sigma^3 = 0.01$. Interactions are given for various values of the bend stiffness parameter, ε.

However, the theory was based on considerations from Edwards−de Gennes theory, in the limit of infinitely long chains. In a previous study[35] we established that finite length effects, as manifested by a sizable barrier, persist with remarkably long polymers. See also the work by van der Gucht et al.[34]

Approaching the Rod-Like Limit. In earlier work,[33] we studied the approach to rod-like behavior for very stiff polymers. In these cases, the persistence length, l_p, approaches the contour length, $L = (r - 1)\sigma$. One may expect that polydispersity effects for semiflexible polymers approaching the rod limit, may be relatively larger than for the systems described above ($l_p \ll L$). Between nonadsorbing walls, for example, one expects to find a population of shorter (more rod-like) polymers between the surfaces, compared with the bulk. On the other hand, for adsorbing walls, one would expect longer polymers between the surfaces, and hence less rod-like behavior. Figure 7 shows the interaction free energy for adsorbing surfaces immersed in a fluid of short, monodispersed polymers. As one approaches more rod-like behavior (by increasing ε), we see a nonmonotonic behavior in the free energy, as has already been described in previous work.[33] It is worthwhile recalling the essential mechanisms behind the nonmonotonic behavior. In the presence of flexible polymers we see the onset of a weak free energy barrier, due to the overlap of adsorbed monomers, as described above. Of course, this occurs at smaller separation now, as the polymers are much shorter ($r = 50$). As ε increases, the position of the barrier, and its magnitude, initially shifts out to larger separation, as expected, but then starts to move inward, as the adsorbed layers become flatter.

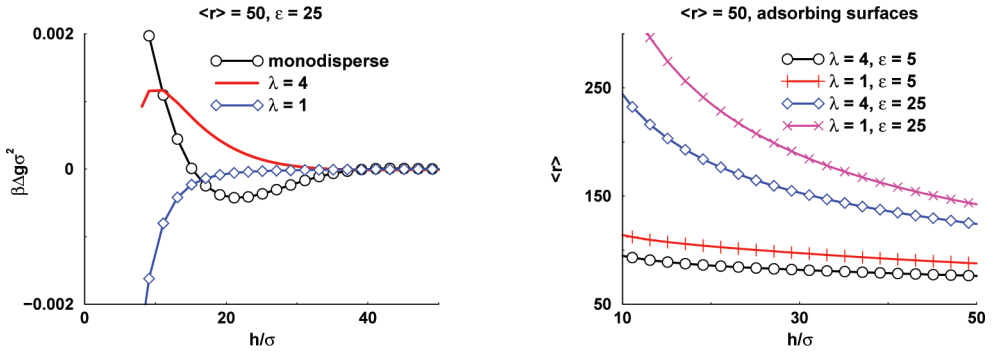

Figure 8. Adsorbing surfaces, immersed in polydisperse polymer solutions, with average length $\langle r \rangle_b = 50$ in the bulk. The bend stiffness parameter is high, $\varepsilon = 25$, which renders the chains rod-like. The bulk monomer concentration is $n_b\sigma^3 = 0.01$. (a) Interaction free energies per unit area. (b) The average chain length, in the intersurface (slit) region.

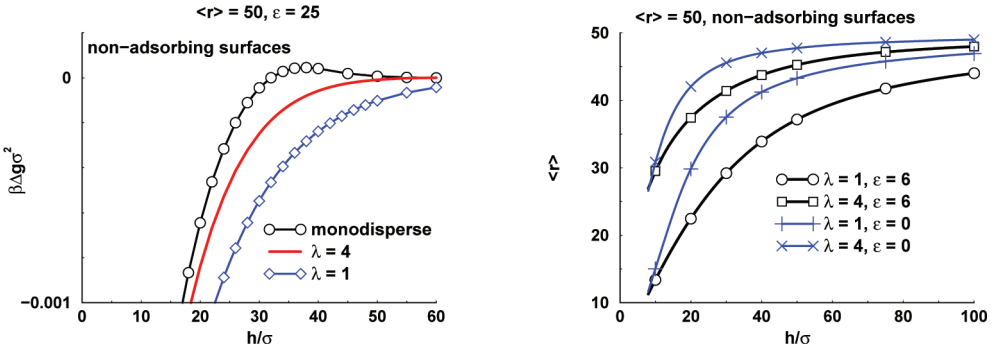

Figure 9. Nonadsorbing surfaces, immersed in polydisperse polymer solutions, with average length $\langle r \rangle_b = 50$ in the bulk. The bend stiffness parameter is high, $\varepsilon = 25$, which renders the chains rod-like. The bulk monomer concentration is $n_b\sigma^3 = 0.01$. (a) Interaction free energies per unit area. (b) The average chain length, in the intersurface (slit) region.

The flattening out of the adsorbed layer is due to the increasing stiffness, which promotes the cooperative adsorption of monomers on the same chain. One also begins to see the onset of a depletion attraction regime at intermediate separations ($h \approx 20\sigma$), which is quite pronounced for the stiffest polymer investigated ($\varepsilon = 25$). This depletion comes from exclusion of nonadsorbed monomers between the surfaces at separations of around the persistence length of the polymer (recall, $l_p \approx \varepsilon$).

As shown in Figure 8a, if the sample containing the stiffest chains is *polydisperse*, we find *dramatically* different interaction free energies. The typical rod-like characteristics of the free energy is suppressed. Instead, we observe a behavior which is reminiscent of longer polymers between adsorbing surfaces, as described earlier. In particular, we see that at intermediate polydispersity ($\lambda = 4$) that the depletion attraction has disappeared and a free energy barrier occurs at a separation that indicates an interaction between two thicker adsorbed layers. For the equilibrium polymer case ($\lambda = 1$), we once again see a purely attractive interaction that is due essentially entirely to bridging. The reason for this behavior is clearly shown in Figure 8b, which indicates a dramatic growth in the average length of polymer population between the surfaces. Thus, the interaction free energy is similar to those found with longer semiflexible polymers. Interactions between nonadsorbing surfaces, immersed in solutions containing rod-like polymers, are presented in Figure 9a. The forces are much stronger in this case, as compared to those seen observed in Figure 1, parts a and b. This is due to the fact that maximal depletion forces in general are stronger with shorter polymers, at a fixed bulk monomer concentration, since the bulk osmotic pressure is higher. For the monodispersed case, we see the occurrence of a slight free energy barrier, at a separation somewhat larger than the persistence length. Here, polymer molecules begin to lose significant configurational free energy due to exclusion by both surfaces simultaneously, but depletion is not yet large enough to create an osmotic attraction. Instead the entropic losses, including those due to an increased excluded volume, cause the free energy to increase slightly, with a resulting barrier. Once the separation is small enough to cause significant depletion, the free energy is monotonically attractive, down to contact. In a widely polydisperse solution, the free energy barrier is absent. This is because long chains are replaced (to some degree) by shorter ones, as the surfaces approach. The subsequent osmotic effect leads to an attraction. This is a similar mechanism to that described above for longer polymers. In this case, however, there is an additional effect from short polymers being more rod-like.

The overall response is illustrated in Figure 9b, which provides the average molecular weight of polymers in the intersurface regime. If we compare with results using flexible polymers, we note that long, flexible polymers are less depleted at large separations, than are stiff molecules. At short separations, though, the greater loss of configurational entropy experienced by the flexible chains, causes them to be depleted more rapidly, and a crossover occurs at $h \approx 10\sigma$. Interestingly, this occurs at approximately the same separation for both degrees of polydispersity, $\lambda = 1.4$, though we cannot see a fundamental reason why this should be the case.

Conclusion

We have developed extended the polymer density functional theory to describe solutions containing polydisperse semiflexible polymers. The method is simple, and applicable to most current versions of PDFT. The theory turns out to be much simpler in

structure than the corresponding PDFT for monodisperse polymers. It is also very easy to implement numerically. We have applied the theory to study interactions between adsorbing and nonadsorbing surfaces. We find that polydispersity effects on depletion attractions in solutions with flexible polymers are relatively small, particularly at high concentrations. This is true also when the chains are moderately stiff. On the other hand, with very stiff (rod-like) polymers, there is a substantial polydispersity effect. This is generated by depletion of longer molecules from the intersurface region, leading to an osmotic attraction.

For adsorbing surfaces, polydispersity has a strong impact on the surface interactions, in solutions containing flexible as well as semiflexible polymers. This is due to the adsorption of longer polymers at the surfaces, leading to increased bridging. Stiffness in the chains, leads to stronger effects at larger separation.

References and Notes

(1) Tuinier, R.; Rieger, J.; de Kruif, C. G. *Adv. Colloid Interface Sci.* **2003**, *103*, 1.
(2) Poon, W. C. K. *J. Phys.: Condens. Matter* **2002**, *14*, R859.
(3) Woodward, C. E. *J. Chem. Phys.* **1991**, *94*, 3183.
(4) Woodward, C. E.; Yethiraj, A. *J. Chem. Phys.* **1994**, *100*, 3181.
(5) Yethiraj, A. *J. Chem. Phys.* **1998**, *109*, 3269.
(6) Forsman, J.; Woodward, C. E.; Freasier, B. C. *J. Chem. Phys.* **2002**, *117*, 1915.
(7) Yu, Y.-X.; Wu, J. *J. Chem. Phys.* **2002**, *117*, 2368.
(8) Yu, Y.-X.; Wu, J.; Xin, Y.-X.; Gao, G.-H. *J. Chem. Phys.* **2004**, *121*, 1535.
(9) Tuinier, R.; Petukhov, A. *Macromol. Theory Simul.* **2002**, *11*, 975.
(10) van der Gucht, J.; Besseling, N. A. M. *Phys. Rev. E* **2002**, *65*, 051801.
(11) van der Gucht, J.; Besseling, N. A. M.; Fleer, G. J. *J. Chem. Phys.* **2003**, *119*, 8175.
(12) van der Gucht, J.; Besseling, N. A. M. *J. of Phys: Condens Matter.* **2003**, *15*, 6627.
(13) van der Gucht, J.; Besseling, N. A. M.; Fleer, G. J. *Macromolecules* **2004**, *37*, 3026.
(14) Scheutjens, J. M. H. M.; Fleer, G. J. *J. Phys. Chem.* **1979**, *83*, 1619.
(15) Roefs, S. P. F. M.; Scheutjens, J. M. H. M.; Leermakers, F. A. M. *Macromolecules* **1994**, *27*, 4180.
(16) Edwards, S. F. *Proc. Roy. Soc.* **1965**, *85*, 613.
(17) de Gennes, P. G. *Rep. Prog. Phys.* **1969**, *32*, 187.
(18) de Gennes, P. G. *Macromolecules* **1982**, *15*, 492.
(19) Sides, S. W.; Fredrickson, G. H. *J. Chem. Phys.* **2004**, *121*, 4974.
(20) Matsen, M. W. *Eur. Phys. J. E* **2006**, *21*, 199.
(21) Cooke, D. M.; Shi, A.-C. *Macromolecules* **2006**, *39*, 6661.
(22) Yang, S.; Tan, H.; Yan, D.; Nies, E.; Shi, A.-C. *Phys. Rev. E* **2007**, *75*, 061803.
(23) Woodward, C. E.; Forsman, J. *Phys. Rev. Lett.* **2008**, *100*, 098301.
(24) Forsman, J.; Woodward, C. E. *J. Chem. Phys.* **2003**, *119*, 1889.
(25) Wertheim, M. S. *J. Chem. Phys.* **1987**, *87*, 7323.
(26) Chiew, Y. C. *Mol. Phys.* **1990**, *70*, 129.
(27) Honnell, K. G.; Hall, C. K. *J. Chem. Phys.* **1991**, *95*, 4481.
(28) Song, Y.; Lambert, S. M.; Prausnitz, J. M. *Macromolecules* **1994**, *27*, 441.
(29) Hooper, J. B.; Pileggi, M. T.; McCooy, J. D.; Curro, J.; Weinhold, J. D. *J. Chem. Phys.* **2000**, *112*, 3094.
(30) Forsman, J.; Woodward, C. E. *J. Chem. Phys.* **2004**, *120*, 506.
(31) Turesson, M.; Forsman, J.; Åkesson, T. *Phys. Rev. E* **2007**, *76*, 021801.
(32) Forsman, J.; Woodward, C. E. *Macromolecules* **2006**, *39*, 1261.
(33) Forsman, J.; Woodward, C. E. *Macromolecules* **2006**, *39*, 1269.
(34) van der Gucht, J.; Besseling, N. A. M.; van Male, J.; Cohen Stuart, M. A. *J. Chem. Phys.* **2000**, *113*, 2886.
(35) Woodward, C. E.; Forsman, J. *Phys. Rev. E* **2006**, *74*, 010801.
(36) Turesson, M.; Woodward, C. E.; Åkesson, T.; Forsman, J. *J. Phys. Chem. B* **2008**, *112*, 9802.
(37) Derjaguin, B. V. *Kolloid Zeits.* **1934**, *69*, 155.
(38) Forsman, J.; Woodward, C. E. *J. Chem. Phys.* **2009**, *131*, 044903.